AECL--10691
COG--92-248

AECL-10691
COG-92-248

ATOMIC ENERGY OF CANADA LIMITED

ÉNERGIE ATOMIQUE DU CANADA LIMITÉE

THERMODYNAMIC BEHAVIOUR OF TELLURIUM AT HIGH TEMPERATURES

COMPORTEMENT THERMODYNAMIQUE DU TELLURIUM À DE HAUTES TEMPÉRATURES

Frank Garisto

Whiteshell Laboratories
Pinawa, Manitoba R0E 1L0

Laboratoires de Whiteshell

September 1992 septembre

AECL RESEARCH

THERMODYNAMIC BEHAVIOUR OF TELLURIUM AT HIGH TEMPERATURES

by

Frank Garisto

Whiteshell Laboratories
Pinawa, Manitoba ROE 1LO
1992

AECL-10691
COG-92-248

COMPORTEMENT THERMODYNAMIQUE DU TELLURIUM À DE HAUTES TEMPÉRATURES

par

Frank Garisto

RÉSUMÉ

Les calculs thermodynamiques servent à déterminer la spéciation chimique du tellurium dans le circuit primaire de caloporteur en situation d'accident de réacteur hypothétique. On détermine la spéciation du tellurium pour diverses valeurs de température, de pression partielle d'oxygène, de concentration de tellurium et de rapport Cs/Te. Les effets de la gaine de Zircaloy et/ou du césium sur la spéciation et volatilité du tellurium présentent un intérêt particulier dans ce rapport.

EACL Recherche
Laboratoires de Whiteshell
Pinawa (Manitoba) ROE 1LO
1992

AECL-10691
COG-92-248

THERMODYNAMIC BEHAVIOUR OF TELLURIUM AT HIGH TEMPERATURES

by

Frank Garisto

ABSTRACT

Thermodynamic calculations are used to determine the chemical speciation of tellurium in the primary heat transport system under postulated reactor accident conditions. The speciation of tellurium is determined for various values of the temperature, oxygen partial pressure, tellurium concentration and Cs/Te ratio. The effects of the Zircaloy cladding and/or cesium on tellurium speciation and volatility are of particular interest in this report.

AECL Research
Whiteshell Laboratories
Pinawa, Manitoba ROE 1LO
1992

AECL-10691
COG-92-248

CONTENTS

1. INTRODUCTION

During postulated nuclear reactor accidents, e.g., loss-of-coolant accidents (LOCAs), the temperature of the fuel may rise, causing failure of the fuel cladding and release of fission products into the primary heat transport system (PHTS). To determine the consequences of such accidents, it is important to understand the behaviour of fission products both in the PHTS and in the reactor containment building.

Many factors can influence the behaviour of fission products after they are released from the fuel. Consequently, the prediction of fission product behaviour during a LOCA is a complex problem. To a large extent, however, fission product behaviour will be determined by the physical and chemical properties of the predominant fission product chemical species formed in the PHTS. Thus, it is important to identify the chemical forms of the radionuclides in the PHTS.

Fuel failures during a LOCA occur predominantly for fuel-sheath temperatures in excess of 1100 K [1]. At these high temperatures, gas-phase chemical reactions are generally fast. Thus, chemical equilibrium should be rapidly attained after the fission products are released from failed fuel into the PHTS. For these cases, fission product chemical speciation can be determined using chemical equilibrium calculations.

This approach has been used in the past to determine the chemical speciation of iodine, cesium, tellurium and ruthenium in the PHTS during a LOCA [2,3]. Kinetic calculations [4] have confirmed, at least for cesium and iodine, the validity of the equilibrium assumption for temperatures down to about 1000 K. In addition, the calculated ruthenium vapour pressures correlate well with the measured rates of release of ruthenium from irradiated fuel [5,6]. This latter agreement allowed us to develop a simple model for predicting ruthenium release rates as a function of temperature and oxygen partial pressure [5].

These previous studies support the use of chemical equilibrium calculations for predicting the behaviour of fission products at high temperatures. In this report, thermodynamic calculations are used to investigate the behaviour of tellurium under reactor accident conditions.

Tellurium is a semi-volatile element with a boiling point of about 1265 K. It is an important fission product in nuclear safety analyses because the ^{132}Te isotope (78 h half-life) is a precursor of the short-lived ^{132}I isotope (2.3 h half-life). The ^{132}I isotope, in turn, represents a potential health hazard during reactor accidents because iodine is biologically active and concentrates in the thyroid.

A CANDU* fuel bundle with a burnup of 180 MW·h/kg U contains about 0.017 moles of tellurium. The ^{132}Te isotope accounts for ~2.5% of the total tellurium reactor inventory. The Te/I and Cs/I ratios in a typical fuel

---

* CANada Deuterium Uranium, registered trademark of AECL.

bundle are about 2 and 10 respectively. Since cesium iodide is thermodynamically very stable, only the excess cesium (with respect to iodine) is available to react with tellurium, i.e., the Cs/Te ratio should be less than 4.5 if iodine is not included in the calculations.

In Reference 2, chemical equilibrium calculations were used to determine the tellurium speciation in the PHTS for various temperatures, tellurium concentrations and oxygen partial pressures. At that time, thermodynamic data were not available for the important cesium-tellurium compounds (e.g., Cs_2Te). Thus, the effect of cesium on the tellurium speciation was not investigated in Reference 2.

The possible interaction of tellurium with the Zircaloy cladding was also ignored in Reference 2. Recent experimental results [7,8,9] indicate, however, that (i) tellurium releases from failed fuel are delayed until the Zircaloy cladding is completely oxidized, and (ii) tellurium reacts with tin (Zircaloy contains ~1.5% by weight Sn) to form tin telluride. Thus, the behaviour of tellurium during reactor accidents can be affected by the presence of the Zircaloy cladding.

The purpose of the present report is to expand the scope of the previous work [2] by studying the chemical speciation and volatility of tellurium in the presence of cesium and/or Zircaloy. The importance of the tellurium-cesium and tellurium-Zircaloy interactions is evident from our calculations. Reactions of tellurium with fission products, other than cesium, are not considered in this report.

2. THERMODYNAMIC DATA FOR TELLURIUM SPECIES

Gibbs energy of formation data, at all temperatures of interest, are required in order to carry out chemical equilibrium calculations. In this report the Gibbs energy of formation, $\Delta_f G°(T)$, with respect to the elements at 298.15 K and 1 bar pressure (1 bar = 100 kPa), is calculated using the formula

$$\Delta_f G°(T) = \Delta_f G°(298) - [T\Phi(T) - 298.15\Phi(298)] \qquad (1)$$

where T is the temperature in kelvin, and $\Phi(T)$ is the Gibbs energy function. With this choice of reference states, Equation (1) must be used to determine the Gibbs energy of formation of all chemical elements in the system. Furthermore, all pressure values must be expressed in bars.

The Gibbs energy function $\Phi(T)$ is defined by

$$\Phi(T) = - [G°(T) - H°(298)]/T \qquad (2)$$

where H°(298) is the enthalpy at 298.15 K. $\Phi(T)$ can also be expressed in terms of the heat capacity (C_p) of the species,

$$\Phi(T) = \Phi(298) + \int_{298}^{T} (C_p^o/T)\, dT - \frac{1}{T} \int_{298}^{T} C_p^o\, dT \qquad (3)$$

where $\Phi(298)$ is equal to the entropy $S^o(298)$ of the species. Values of $\Phi(T)$ are available in the literature for many compounds. It was found convenient to fit the $\Phi(T)$ values to the following six-parameter function of temperature:

$$g(T) = A_0 + A_{1n}\, \ln(X) + A_{-2}/X^2 + A_{-1}/X + A_1 X + A_2 X^2 \qquad (4)$$

where

$$X = T \times 10^{-4} \quad .$$

The tellurium species that are included in our equilibrium calculations are listed in Table 1. The parameters needed to calculate values of $\Phi(T)$ for these species are given in Table 2. For a condensed species, e.g., Te(c), separate sets of parameters are required for different temperature ranges. This usually reflects a change in the state of the species, e.g., a solid-to-liquid transition. For some species, e.g., $Zr_5Te_4(s)$, the range of validity of the parameters in Table 2 does not include all temperatures of interest. Nevertheless, the parameter values in Table 2 were used to obtain extrapolated values of $\Phi(T)$. Although the uncertainties in the extrapolated values of $\Phi(T)$ may be large, the largest contribution to the uncertainty in $\Delta_f G^o(T)$ should still result from the uncertainty in the value of $\Delta_f G^o(298)$.

The thermodynamic data for most of the tellurium species listed in Table 1 were obtained from the compilation of Cordfunke and Konings [10]. The thermodynamic data for Te_2O_2 were taken from Mills [11], except that the enthalpy of formation was updated to reflect the revised data for TeO [10]. However, data for some important tellurium species, e.g., Cs_2Te and $Zr_5Te_4(s)$, are not available from these two sources. The origin of these thermodynamic data is discussed below. Thermodynamic data for the other species that are present in the PHTS during a LOCA, e.g., H_2O and H_2, were obtained from the compilations of Cordfunke and Konings [10] or Glushko et al. [12].

A detailed discussion of the origin of the thermodynamic data for $Cs_2Te(g)$, $Zr_5Te_4(s)$, Sn(in Zr) and SnTe(l) is given below. (Readers who are not interested in these details may proceed directly to Section 3.)

$Cs_2Te(g)$

Values of $\Phi(T)$ for $Cs_2Te(g)$ were calculated in the rigid rotator - harmonic oscillator approximation using statistical thermodynamic methods [13]. Since the spectroscopic and molecular constants needed for this calculation were not available in the literature, they were estimated from the

TABLE 1

THERMODYNAMIC DATA FOR THE TELLURIUM SPECIES INCLUDED IN THE CALCULATIONS, Sn(in Zr) AND AUXILIARY SPECIES

Species[1]	$S^\circ(298.15)$ ($J \cdot K^{-1} \cdot mol^{-1}$)	$\Delta_f G^\circ(298.15)$ ($kJ \cdot mol^{-1}$)
Te	182.7	169.7
Te_2	258.9	115.3
H_2Te	228.5	85.2
TeO_2	272.9	-60.3
TeO	235.5	67.0
Te_2O_2	327.3	-80.8
Te(c)	49.2	0.0
TeO_2(c)	69.9	-266.0
$TeO(OH)_2$	332.6	-383.8
Cs_2Te(c)	185.1	-351.8
Cs_2Te	350.9	-173.6
Cs_2TeO_3(s)	232.0	-905.7
Cs_2TeO_4(s)	233.0	-1001.1
$Cs_2Te_2O_5$(s)	302.0	-1210.6
$Cs_2Te_4O_9$(s)	442.0	-1782.7
Zr_5Te_4(s)	378.0	-717.2
$ZrTe_2$(s)	124.2	-290.2
SnTe(c)	104.4	-60.7
SnTe	264.1	112.2
Sn(in Zr)	25.5	-126.9
Sn(c)	51.2	0.0
Zr(s)	39.0	0.0

[1] The state of a species is denoted by the letters: c (condensed state, solid or liquid), s (solid), l (liquid) and g (gas). The gaseous state is implied if the state of the species is not explicitly indicated.

corresponding data for Cs_2O [14]. Cs_2O is a non-linear molecule with a Cs–O–Cs bond angle of 140°. The vibrational frequencies of Cs_2O are 305, 60 and 455 cm^{-1}.

The valence force approximation [15] and the Cs_2O data were used to estimate the vibrational frequencies of Cs_2Te and the Cs–Te–Cs bond angle. This calculation should give good estimates for the shifts in vibrational frequencies caused by the difference in the atomic masses of oxygen and tellurium. However, such a simple calculation cannot be expected to predict the shifts in vibrational frequencies caused by differences in the Cs-Te and Cs-O bond strengths.

TABLE 2

PARAMETERS NEEDED TO CALCULATE $\Phi(T)$ FOR VARIOUS SPECIES ($J \cdot K^{-1} \cdot mol^{-1}$)

Species	Temperature Range (K)	A_0	A_{1n}	A_{-2}	A_{-1}	A_1	A_2
Te	298-3000	230.081	18.7006	1.0538E-03	0.50066	11.4719	0.0000
Te_2	298-3000	366.261	45.3733	-6.7800E-03	1.78118	-2.0254	0.0000
H_2Te	298-3000	330.585	44.8262	-9.0077E-03	1.92720	27.9014	0.0000
TeO_2	298-3000	407.208	56.2665	-6.2585E-03	2.09383	5.3361	0.0000
TeO	298-3000	335.163	39.2872	1.0720E-03	1.11088	-2.9656	0.0000
Te_2O_2	298-1900	526.237	81.7973	-5.5957E-03	2.81970	3.9611	0.0000
Te(c)	298- 723	115.757	26.5444	0.0000E+00	0.79629	0.0000	0.0000
	723-1300	153.379	34.3220	0.0000E+00	-0.44613	0.0000	0.0000
TeO_2(c)	298-1004	218.155	63.4307	-4.1270E-03	2.26440	108.5380	0.0000
	1004-2000	312.602	106.5600	0.0000E+00	3.22810	55.5925	0.0000
$TeO(OH)_2$	298-3000	581.795	106.5300	-1.4930E-02	4.18600	46.8451	0.0000
Cs_2Te(c)	298-1083	356.351	71.0132	0.0000E+00	2.22440	120.5230	0.0000
	1083-1500	432.326	101.0000	0.0000E+00	2.62880	0.0000	0.0000
Cs_2Te	298-3000	496.581	58.1997	-4.6991E-04	1.76667	0.0000	0.0000
Cs_2TeO_3(s)	298-1084	484.353	109.9480	0.0000E+00	3.63470	401.1110	0.0000
Cs_2TeO_4(s)	298- 920	466.648	108.7460	0.0000E+00	3.83270	664.1500	0.0000
$Cs_2Te_2O_5$(s)	298- 713	772.101	199.2270	-1.0884E-02	6.94230	306.2390	0.0000
$Cs_2Te_4O_9$(s)	298- 823	1018.422	254.6780	0.0000E+00	8.54010	1065.2150	0.0000
$ZrTe_2$(s)	298-1500	304.954	73.4840	-1.0092E-03	2.30082	45.2465	37.2345
Zr_5Te_4(s)	900-1100	921.292	220.7000	0.0000E+00	6.74820	189.0000	0.0000
SnTe(c)	298-1079	224.417	48.9570	2.2570E-05	1.50320	50.7050	0.0000
	1079-2000	283.800	63.5000	0.0000E+00	-0.81651	0.0000	0.0000
SnTe	298-3000	356.960	37.0364	0.0000E+00	1.10958	2.3643	0.0000
Sn(in Zr)	1600-2000	105.522	25.1840	4.0940E-03	-0.18369	10.5250	-2.7170
Sn(c)	298- 505	142.649	34.2970	-1.2305E-03	1.01683	-149.7850	846.5670
	505-4700	131.192	25.1840	4.0940E-03	-0.18369	10.5250	-2.7170
Zr(s)	298-1140	94.673	23.5840	-5.1900E-04	0.78250	50.0400	0.0000
	1140-2133	83.068	9.9290	3.4961E-02	-1.68500	57.6350	0.0000

Using 0.30 nm for the Cs-Te bond length and the selected values of the Cs_2O vibrational frequencies, we find that, to obtain consistent values for the Cs_2Te vibrational frequencies, the Cs–Te–Cs bond angle must equal 120°. The calculated vibrational frequencies of Cs_2Te are equal to 199, 49 and 156 cm^{-1}. With these data, we find the following for Cs_2Te(g): $S°(298) = 350.87\ J \cdot K^{-1} \cdot mol^{-1}$, $C_p°(298) = 57.16\ J \cdot K^{-1} \cdot mol^{-1}$, and $[H°(298) - H°(0)] = 15.25\ kJ \cdot mol^{-1}$. Values of $\Phi(T)$ for Cs_2Te can be calculated using the data in Table 2.

Cordfunke et al. [16] measured the vapour pressure of Cs_2Te(s) in the temperature range from 850 to 1000 K. Let us assume that only Cs_2Te contributes significantly to the measured vapour pressure. Using a third-law

analysis of the vapour pressure data, we find that the enthalpy of sublimation of cesium telluride is equal to 227 $kJ \cdot mol^{-1}$ at 298.15 K. A second law analysis of the same data, however, gives 150 $kJ \cdot mol^{-1}$ for the enthalpy of sublimation. This large difference suggests that the analysis is not correct. The assumption that Cs_2Te is the only important gas-phase species is probably not valid, and other cesium-tellurium species, e.g., CsTe and Cs_2Te_2, contribute significantly to the measured $Cs_2Te(s)$ vapour pressure [17].

Although the thermodynamic data for $Cs_2Te(g)$ derived from the third-law analysis are probably not accurate, they have been included in our calculations because (i) these are the only available data; (ii) the calculated $Cs_2Te(s)$ vapour pressures are within a factor of 3 of the experimentally measured vapour pressures [16] (see Table 3); and (iii) the volatility of $Cs_2Te(s)$ would be underestimated if $Cs_2Te(g)$ is omitted from the database. That is, ignoring the cesium-tellurium gas-phase species does not give a conservative approximation. The species $Cs_2Te(g)$ should perhaps be considered as representing a mixture of cesium-tellurium gas-phase species rather than a single species.

TABLE 3

$Cs_2Te(s)$ VAPOUR PRESSURES

Temperature (K)	Vapour Pressure (Pa)	
	Calculated	Measured [16]
852.3	0.35	0.43
868.4	0.27	0.64
877.9	0.38	0.79
894.3	0.64	1.00
912.0	1.11	1.37
935.1	2.20	1.99
935.2	2.21	1.78
946.8	3.08	3.16
961.3	4.60	3.49
962.2	4.71	3.59
980.4	7.66	4.82
999.8	12.60	7.54

$Zr_5Te_4(s)$

The amount of tellurium in a fuel element is very small compared with the amount of Zircaloy. Thus, the tellurium in the fuel gap should dissolve in the Zircaloy. However, data for the activity coefficient of Te in Zr are not available. Thus, $Zr_5Te_4(s)$, the Zr-Te compound with the largest Zr/Te ratio [18], was included in our calculations to represent the product of the Zr-Te reaction. Although the $Zr_3Te(s)$ phase may also exist [10], even estimated thermodynamic data for this compound are not available.

Since the thermodynamic properties of $Zr_5Te_4(s)$ have not been measured, estimated values were used in our calculations. An estimate of the partial pressure of Te_2, $p(Te_2)$, in equilibrium with both Zr(s) and $Zr_5Te_4(s)$ (at 973 K) is found in Figure 5 of Yamanaka et al. [18]. (These authors did not find the $Zr_3Te(s)$ phase at 973 K.) Using $p(Te_2) = 2.14 \times 10^{-15}$ Pa, we find that the Gibbs energy of formation of $Zr_5Te_4(s)$ at 973 K is -1086 kJ·mol^{-1}. Gibbs energy function values for $Zr_5Te_4(s)$ were then calculated by (i) using the method of Yamanaka et al. [19] to estimate the entropy of $Zr_5Te_4(s)$, $S°(298) = 378$ J·K^{-1}·mol^{-1}; and (ii) approximating the heat capacity of $Zr_5Te_4(s)$ using the following equation:

$$C_p°(Zr_5Te_4(s),T) = 2C_p°(ZrTe_2(s),T) + 3C_p°(Zr(s),T) \qquad (5)$$

We find, using Equation (1), that $\Delta_fG°(Zr_5Te_4(s),298) = -717.8$ kJ·mol^{-1}.

Sn(in Zr)

Vapour pressure measurements [20] and theoretical calculations [21] show that the enthalpy of dissolution of tin in zirconium is large and negative. Thus, the Gibbs energy of solution of tin in zirconium is needed in order to study the formation of tin telluride in the PHTS. This datum can be obtained from the activity coefficient of tin in zirconium.

Zee et al. [20] used a modified evaporation method to determine the solute diffusivity and chemical activity of Sn in Zr-based alloys. The activity coefficient of tin in zirconium, $\gamma_{Sn}(T)$, based on our selected thermodynamic values for Sn(c) is given by

$$\gamma_{Sn}(T) = 21.9 \exp(-16\,180/T) \quad , \quad 1600 < T < 2000 \text{ K} \qquad (6)$$

Since $\gamma_{Sn}(T)$ has been measured for a relatively narrow temperature range, the values of $\gamma_{Sn}(T)$ for temperatures less than 1600 K were obtained by extrapolating the formula in Equation (6) to lower temperatures.

The Gibbs energy of formation of Zircaloy (Zry) at temperature T, $\Delta_fG°(Zry,T)$, can be written in the form

$$\Delta_fG°(Zry,T) = X_{Zr}[\Delta_fG°(Zr(s),T) + RT \ln(X_{Zr})] + X_{Sn}[\Delta_fG°(Sn(c),T) + RT \ln(X_{Sn}\gamma_{Sn}(T))] \qquad (7)$$

where X_{Sn} is the mole fraction of Sn in Zircaloy and $X_{Zr} = (1 - X_{Sn})$. In Equation (7), $\Delta_fG°(Zry,T)$ is written in terms of the thermodynamic properties of Zr(s) and Sn(c), i.e., the reference states are the pure metals Zr(s) and Sn(c). However, the reference states Zr(s) and Sn(in Zr) can also be used to describe the thermodynamic properties of Zircaloy, i.e.,

$$\Delta_f G^\circ(Zry,T) = X_{Zr}[\Delta_f G^\circ(Zr(s),T) + RT \ln(X_{Zr})] + X_{Sn}[\Delta_f G^\circ(Sn(\text{in } Zr),T) + RT \ln(X_{Sn})] \quad (8)$$

where

$$\Delta_f G^\circ(Sn(\text{in } Zr),T) = \Delta_f G^\circ(Sn(c),T) + RT \ln(\gamma_{Sn}(T)) \quad (9)$$

is the Gibbs energy of formation of Sn(in Zr). In Equation (8), Zircaloy is represented as an ideal solution of the two reference materials Zr(s) and Sn(in Zr). We must use this latter representation because our chemical equilibrium program can handle only ideal solutions.

SnTe(l)

Cordfunke and Konings [10] list the thermodynamic properties of SnTe(s) and SnTe(g). We estimated the Gibbs energy function values for SnTe(l) using Equation (3). The heat capacity of SnTe(l), assumed to be temperature-independent, was estimated to be 63.3 $J \cdot K^{-1} \cdot mol^{-1}$ using the approximate methods found in Kubaschewski and Alcock [22].

3. THERMODYNAMIC BEHAVIOUR OF TELLURIUM AT HIGH TEMPERATURES

In this section chemical equilibrium calculations are used to determine the chemical speciation of tellurium under various reactor accident conditions. The tellurium species included in the calculations are listed in Table 1. The high-temperature Gibbs energies of formation for all chemical species were calculated using the procedure outlined in Section 2.

Our computer program CHEMEQ was used to perform the chemical equilibrium calculations described in this report. CHEMEQ uses an improved version of the Villars-Cruise algorithm [23]. The Villars-Cruise algorithm is based on the stoichiometric formulation [23] of the chemical equilibrium problem and on the conservation of elemental abundances. It is particularly efficient in determining the equilibrium composition for a system composed of a gas phase in contact with pure condensed chemical species. Because the algorithm is based on the conservation of elemental abundances, CHEMEQ can only determine the chemical equilibrium composition of a closed system.

The results of our calculations are presented in the form of tellurium speciation versus temperature diagrams (see Figure 1). The ordinate of a tellurium speciation diagram gives the abundance of a particular tellurium species, at equilibrium, as the fraction of the total tellurium in the system. Consequently, both gas-phase and condensed-phase (solid or liquid) species can be included on a single graph.

The vapour pressure, $p(Y_nTe_m)$, of the tellurium gas-phase species Y_nTe_m, at equilibrium, can be calculated from the fraction, f, found in the chemical speciation diagrams by using the formula

$$p(Y_nTe_m) = P_T(N_{Te}/N_T)f(Y_nTe_m)/m \qquad (10)$$

where P_T is the total system pressure, N_{Te} is the total abundance of tellurium in the system, and N_T is the total number of moles of gas in the system. For the case shown in Figure 1, $N_T \simeq 2$, the number of moles of steam in the system, $N_{Te} = 0.02$ and $P_T = 12$ bar.

The temperature, pressure, tellurium abundance, and (initial) H_2/H_2O or O_2/H_2O ratio must be specified for each equilibrium calculation. Values for some of these parameters, e.g., pressure, can be obtained from thermal-hydraulic calculations. Other parameters, e.g., tellurium abundance, are varied from calculation to calculation to study the behaviour of tellurium for different accident scenarios.

The maximum tellurium concentration considered in this report is equivalent to the release of the tellurium inventory of one fuel bundle into the coolant volume of a CANDU fuel channel. This maximum release is not intended to simulate any particular accident, but is simply a convenient reference case for subsequent calculations.

The pressure, temperature and coolant volume (20.5 L) of a CANDU fuel channel can be used, along with the ideal gas law ($pV = nRT$), to determine the quantity of steam in a fuel channel during a LOCA. Therefore, in

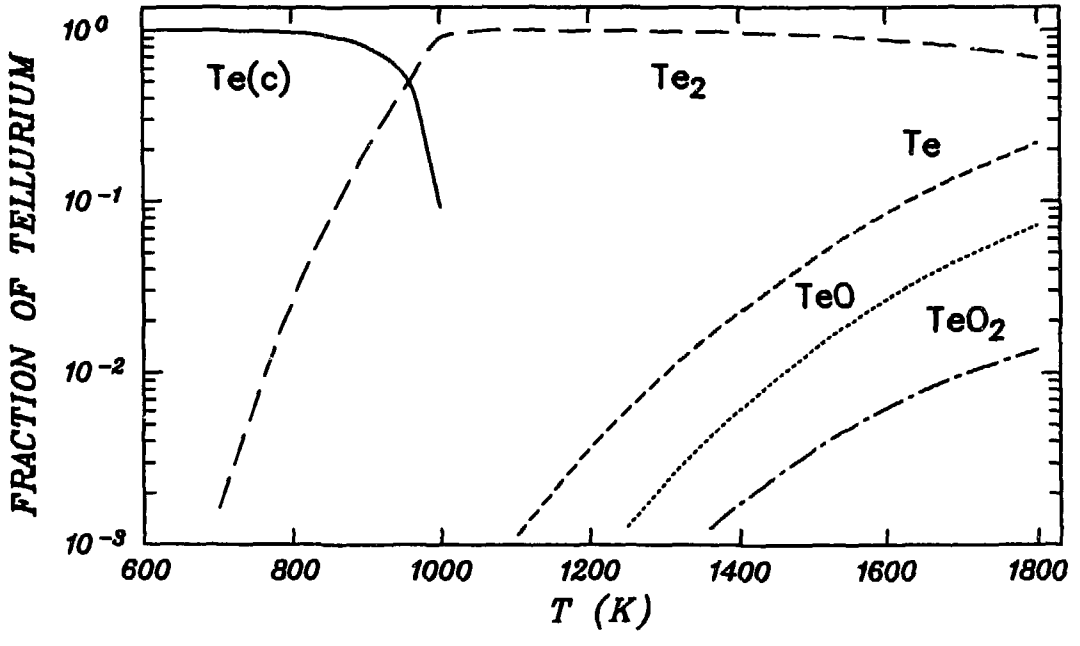

FIGURE 1: Tellurium Speciation Diagram for a System Containing 0.02 mol of Tellurium and 2 mol of Steam at 12-bar Pressure

principle, the number of moles of steam in the fuel channel is temperature-dependent. However, preliminary calculations showed that, for the temperature range of interest, the amount of steam in the fuel channel does not affect the tellurium speciation to any significant degree. Thus, for simplicity, the amount of steam in the fuel channel is kept constant for all temperatures.

At high temperatures, the production of hydrogen by the Zircaloy-steam reaction ensures that reducing-steam conditions are maintained in the PHTS during a LOCA. Neutral-steam conditions (the H/O ratio in the system is approximately 2.0) should prevail at lower temperatures since the Zircaloy-steam reaction occurs at appreciable rates [24] only for fuel sheath temperatures above 1200 K. For most LOCA scenarios, oxidizing-steam conditions should not occur in the PHTS because the high pressure in the PHTS prevents invasion of the PHTS by the containment building atmosphere.

3.1 SUMMARY OF PREVIOUS THERMODYNAMIC CALCULATIONS (REFERENCE 2)

For comparison purposes and completeness, we shall first summarize the results of our previous thermodynamic calculations [2]. The figures presented in this report are not identical to those in Reference 2 because the thermodynamic data for some species, e.g., TeO, have been updated.

Under neutral- or reducing-steam conditions (see Figures 1 and 2), Te(c) and Te_2 are the most important tellurium species at low and high temperatures respectively. At very high temperatures Te_2 dissociates and Te becomes the predominant tellurium species.

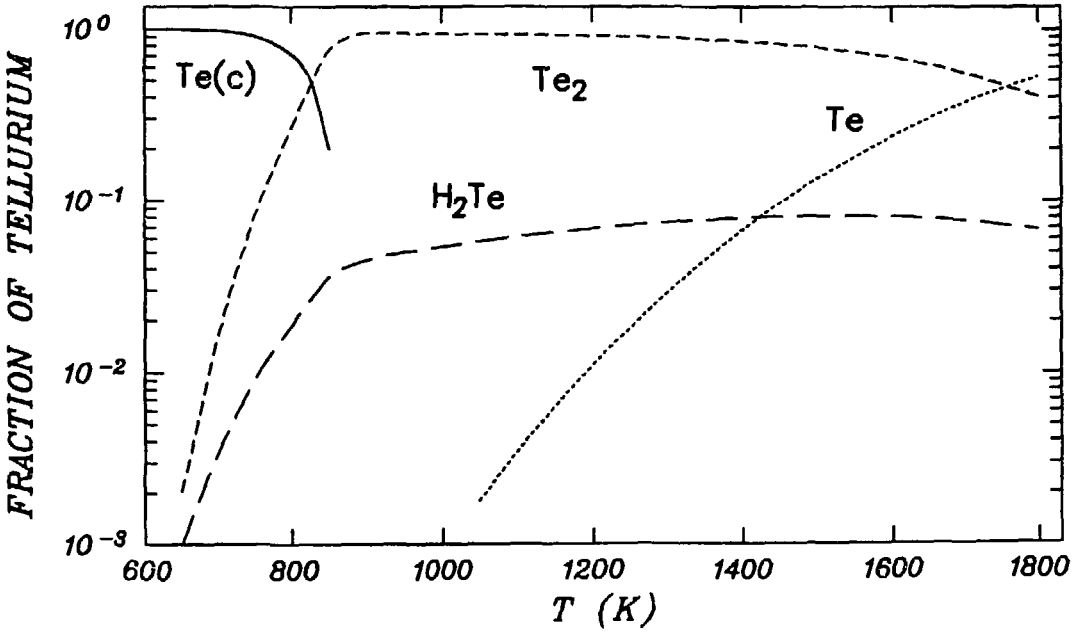

FIGURE 2: Tellurium Speciation Diagram for a System Containing 0.002 mol of Tellurium, 1 mol of Steam and 1 mol of Hydrogen at 12-bar Pressure

Hydrogen telluride, H_2Te, can become an important tellurium species for reducing-steam conditions. Although H_2Te is unstable and rapidly decomposes into its constituent elements [25] at low temperatures ($T < 900$ K), it can become an important tellurium species at intermediate temperatures and large H_2/Te ratios (see Figure 2). This can be understood in terms of the equilibrium

$$H_2 + 1/2Te_2 = H_2Te \qquad (11)$$

The equilibrium constant for this reaction, K_{11}, is given by

$$K_{11} = p(H_2Te)/([p(Te_2)]^{1/2}p(H_2)) \qquad (12)$$

This equation shows that the ratio $p(H_2Te)/p(Te_2)$ increases if $p(H_2)$ is increased, i.e., an increase in $p(H_2)$ shifts the equilibrium of Reaction (11) to the right (Le Chatelier's principle). In addition, for constant $p(H_2)$, decreasing $p(Te_2)$ by a factor of, say, 10 would decrease the value of $p(H_2Te)$ by only a factor of $(10)^{1/2}$, making H_2Te relatively more important at low Te_2/H_2 ratios. Thus, the relative amount of H_2Te in the system increases if the total tellurium abundance is decreased [2].

Under oxidizing-steam conditions, Figure 3 shows that $TeO_2(c)$ and TeO_2 are the predominant tellurium species at low and high temperatures respectively. The volatility of $TeO_2(c)$ is enhanced in the presence of steam as a result of the formation of $TeO(OH)_2$ [26].

3.2 TELLURIUM BEHAVIOUR IN THE PRESENCE OF CESIUM

The presence of cesium can affect the speciation and volatility of tellurium as a result of the formation of cesium-tellurium compounds [10,27]. Iodine, on the other hand, affects the tellurium speciation only indirectly (by tying up cesium and reducing the "effective" Cs/Te ratio), because tellurium iodide compounds are not very stable. Since the Cs/I ratio in irradiated fuel is about 10, the presence of iodine does not have a large effect on the Cs/Te ratio. Consequently, iodine is not included in our chemical equilibrium calculations.

As previously discussed in Section 2, the Gibbs energy of formation for $Cs_2Te(g)$ listed in Table 1 is probably not accurate. Nevertheless, we have used this value in our calculations because (i) no other data are available for $Cs_2Te(g)$, or any other cesium telluride gas-phase species; (ii) omitting all cesium-telluride gas-phase species from the database does not produce a conservative approximation; and (iii) cesium tellurides have been found on the cladding of irradiated fuel [28,29] and have been detected in fission product release experiments [8,30]. In this report, the $Cs_2Te(g)$ species could perhaps be viewed as representing the mixture of cesium-telluride gas-phase species in the vapour phase above $Cs_2Te(c)$.

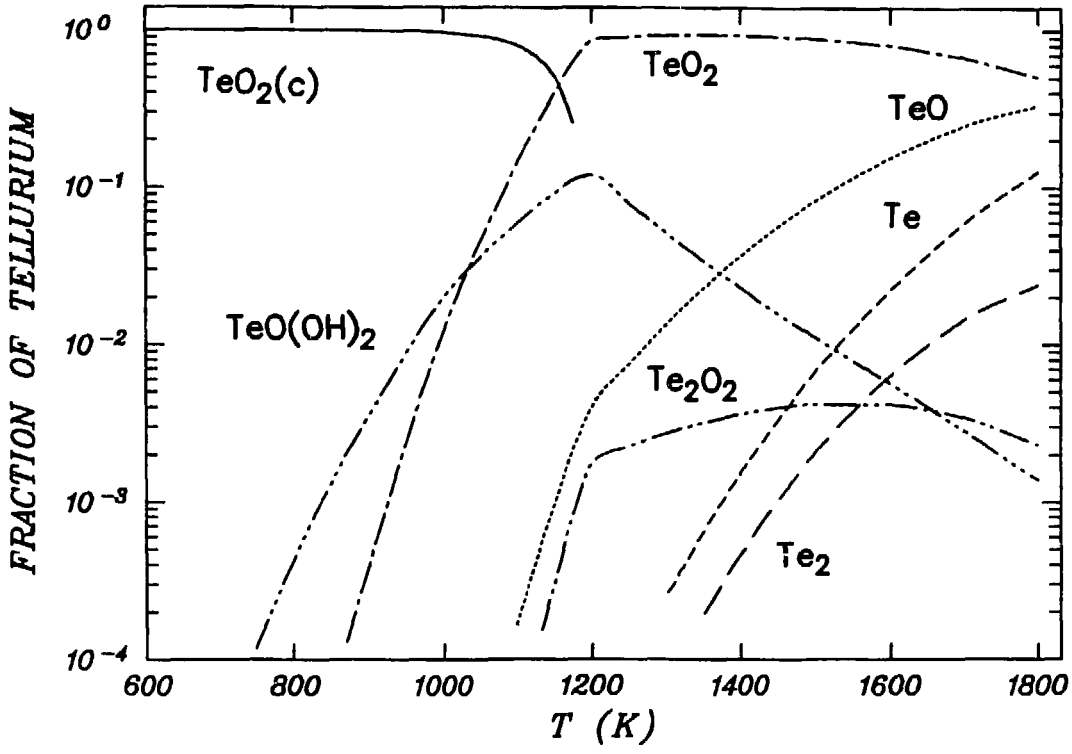

FIGURE 3: Tellurium Speciation Diagram for Release of 0.002 mol of Tellurium into a 50% Steam-Air Atmosphere (0.08 mol of Steam) at 1-bar Pressure

The tellurium speciation diagram for release of tellurium (0.02 mol) and cesium (Cs/Te = 4) into a steam atmosphere is shown in Figure 4. $Cs_2Te(c)$ is formed at the lower temperatures and Cs_2Te is an important tellurium gas-phase species, especially at intermediate temperatures. The formation of $Cs_2Te(c)$ decreases the volatility of tellurium for temperatures less than about 1300 K. At temperatures above 1600 K, Cs_2Te is unstable, and Te and Te_2 become the important tellurium species, i.e., the presence of cesium does not significantly affect the tellurium speciation or volatility at high temperatures.

The decrease in the Cs_2Te concentration with temperature can be understood in terms of the reaction

$$Cs_2Te + 2H_2O = 2CsOH + H_2 + 1/2Te_2 \qquad (13)$$

The temperature dependence of $\Delta_r G$, the Gibbs energy of reaction, can be approximated using the equation

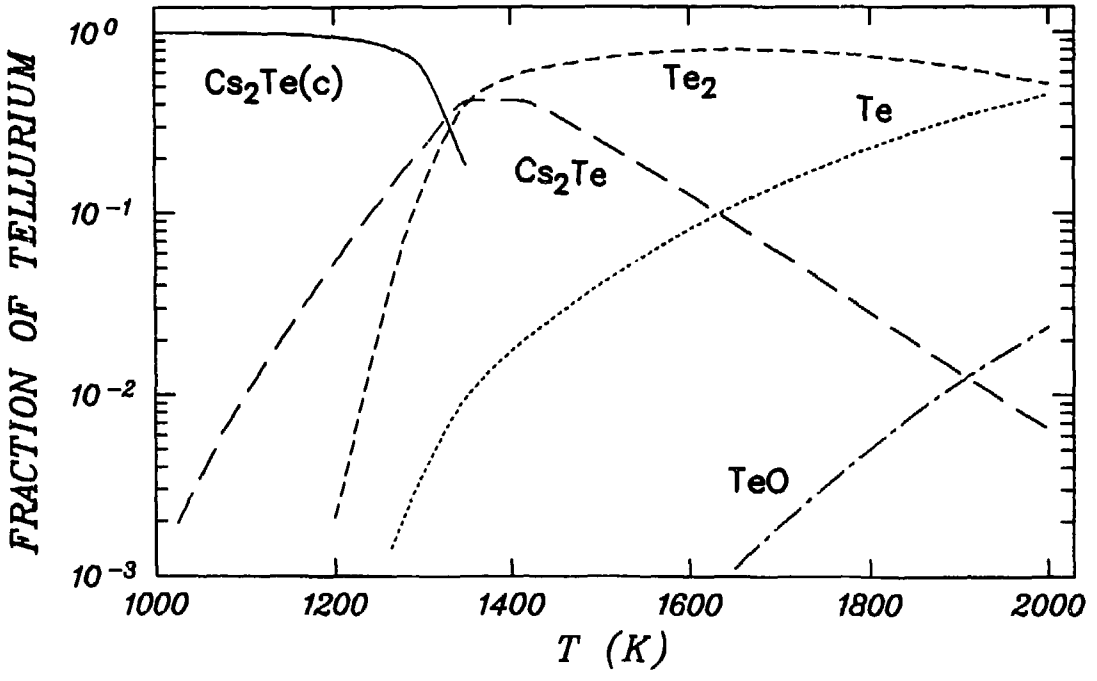

FIGURE 4: Tellurium Speciation Diagram for a System Containing 0.02 mol of Tellurium, Cesium (Cs/Te = 4) and 2 mol of Steam at 12-bar Pressure

$$\Delta_r G = \Delta_r H(298) - T\Delta_r S(298) \qquad (14)$$

where $\Delta_r H(298)$ and $\Delta_r S(298)$ are the enthalpy and entropy changes of the reaction at 298.15 K. Since $\Delta_r S$ for Reaction (13) is large and positive, $\Delta_r G$ for Reaction (13) decreases with temperature, i.e., the stability of Cs_2Te decreases as the temperature increases.

The effect of cesium on the tellurium speciation is more important under reducing-steam conditions. This is illustrated in Figure 5a (cf. Figure 4), which shows the tellurium speciation in a 50% steam-hydrogen mixture. (The notation 60% steam-hydrogen mixture, for example, is used to denote a mixture in which the mole fractions of steam and hydrogen are 0.60 and 0.40 respectively.) In this case, Cs_2Te remains an important species even at high temperatures. The stabilization of cesium telluride in the presence of H_2 can also be understood in terms of Reaction (13), i.e., the equilibrium in Equation (13) is shifted to the left as the H_2/H_2O ratio increases. (In the absence of steam, e.g., in the fuel-cladding gap, CsOH cannot form and cesium telluride could be stable at even higher temperatures.) The effect of decreasing the fission product (Cs and Te) abundances in the system is shown in Figure 5b. The relative importance of Cs_2Te decreases as the fission product abundances in the system are decreased.

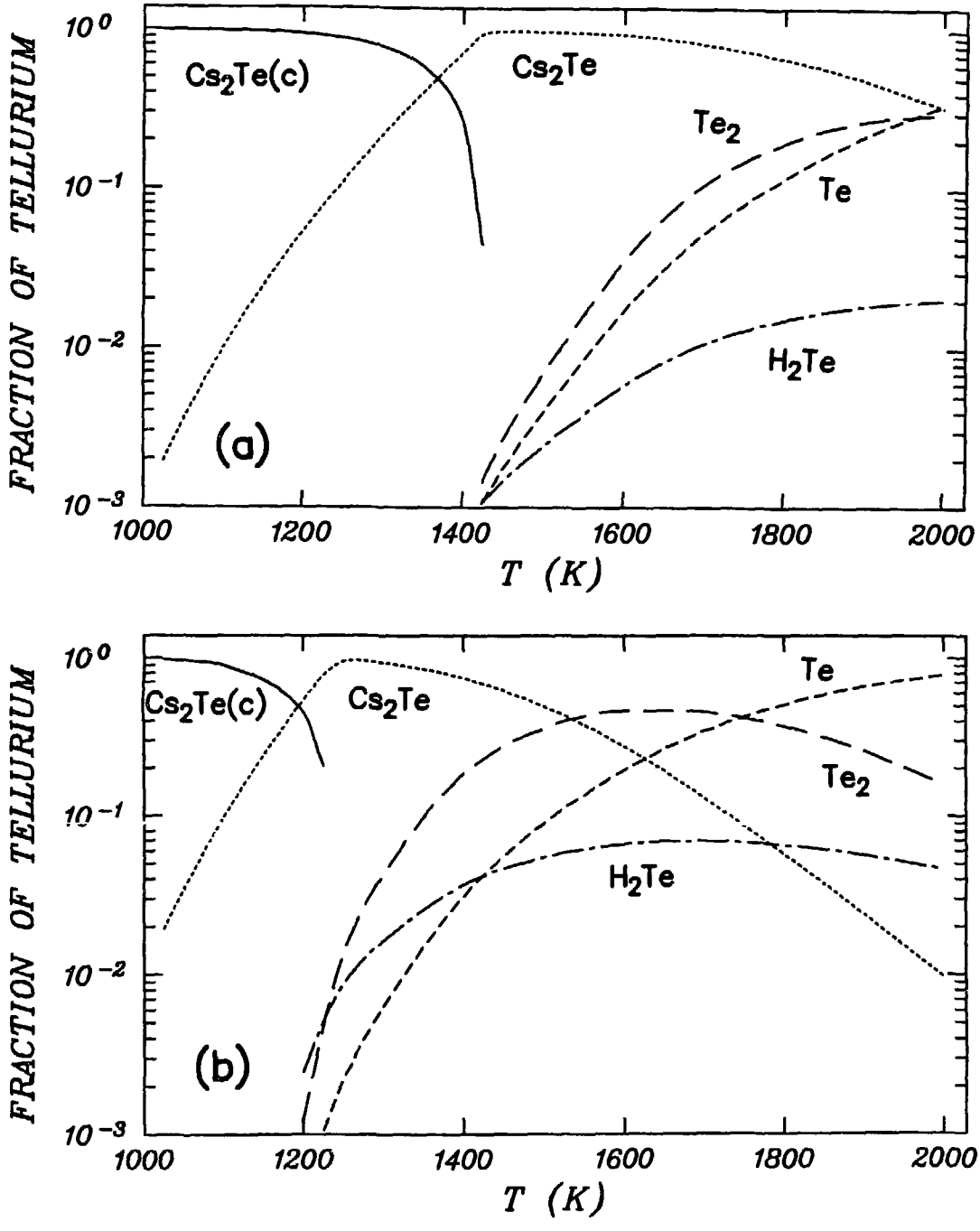

FIGURE 5: Tellurium Speciation Diagram for Release of Tellurium and Cesium (Cs/Te = 4) into a 50% Steam-Hydrogen Atmosphere (1 mol of Steam) at 12-bar Pressure: (a) 0.02 mol of Tellurium and (b) 0.002 mol of Tellurium

In nuclear safety studies, the total volatility of a chemical element is often used to estimate risk factors for reactor accidents. Our calculations show that, at high temperatures, the presence of cesium will affect the chemical speciation of tellurium but not the volatility of tellurium, since all the tellurium in the system is in the gas phase above ~1300 K both in the presence and absence of cesium. At lower temperatures the volatility of tellurium, in the presence of cesium, would be controlled by the vapour pressure of $Cs_2Te(c)$. The vapour pressure of $Cs_2Te(c)$, as a function of temperature, can be calculated using the equations in Table 4.

TABLE 4

VAPOUR PRESSURES OF SOME TELLURIUM COMPOUNDS

$\ln(P(bar)) = A + B/T + C \ln(T)$

Reaction	Temperature Range (K)	Parameter Values		
		A	B	C
$Cs_2Te(s) = Cs_2Te$	300-1083	43.316	-28 521	-3.441
$Cs_2Te(l) = Cs_2Te$	1083-2000	55.183	-28 435	-5.153
$SnTe(s) = SnTe$	300-1079	33.959	-27 214	-2.183
$SnTe(l) = SnTe$	1079-2000	37.469	-24 137	-3.095
$TeO_2(s) = TeO_2$	300-1004	41.595	-32 837	-2.536
$TeO_2(l) = TeO_2$	1004-1800	79.832	-34 730	-7.797
$2Te(c) = Te_2$	300- 723	30.567	-20 115	-1.687
$2Te(l) = Te_2$	723-1800	34.374	-16 729	-2.976
$Te(c) = Te$	300- 723	20.715	-25 404	-0.693
$Te(l) = Te$	723-1800	23.977	-23 811	-1.523
$1/2Zr_5Te_4(s) = 5/2Zr(s) + Te_2$	300-2100	19.287	-62 768	0.0
$1/4Zr_5Te_4(s) = 5/4Zr(s) + Te$	300-2100	16.159	-46 796	0.0

3.3 TELLURIUM BEHAVIOUR IN THE PRESENCE OF ZIRCALOY

The tellurium speciation diagrams presented in the previous sections describe the chemical speciation of tellurium in the absence of tellurium-Zircaloy interactions. In this section, we investigate two (limiting) scenarios in which Zircaloy can affect the behaviour of tellurium: (i) a scenario in which the zirconium in the cladding is completely oxidized, and (ii) a scenario in which the zirconium is unoxidized.

A tin-rich Sn-Zr alloy is formed during the oxidation of Zircaloy [7]. The tellurium in the PHTS can react with this tin-rich alloy to form tin tellurides. The behaviour of tellurium under these conditions was investigated by including the following tin species in the chemical equilibrium calculations: SnTe(c), SnTe, Sn(c), Sn, $SnO_2(c)$, and SnO_2. It should be noted that formation of tin telluride is not thermodynamically favoured if

the Zircaloy remains unoxidized, because the activity of Sn in Zr is small (see Equation (6)), and the thermodynamic stability of SnTe(c) is not very pronounced (see Table 2).

In the presence of steam, Zircaloy is thermodynamically unstable with respect to formation of ZrO_2(s). Thus, the thermodynamic calculations that include (unoxidized) Zircaloy were carried out in the absence of steam. These calculations are meant to model the behaviour of tellurium in the fuel-cladding gap before fuel failure. Of particular interest is the stability of the zirconium telluride compounds in the fuel gap. Since the zirconium tellurides are unstable in the presence of steam, their formation in the gap could explain the delay in the release of tellurium from fuel [7,8,9] until the cladding is oxidized.

3.3.1 Tellurium Behaviour in the Presence of Tin

The chemical speciation of tellurium in a 50% steam-hydrogen mixture in the presence of tin (but no cesium) is shown in Figure 6. SnTe(c) is formed at low temperatures and SnTe is important at high temperatures. (The vapour pressure of SnTe(c) can be calculated using the equations in Table 4.) The formation of SnTe(c) decreases the volatility of tellurium (cf. Figures 2 and 6) since SnTe(c) is less volatile than Te(c). The tellurium speciation diagram in Figure 6 is not affected much by a change in the H_2/H_2O ratio.

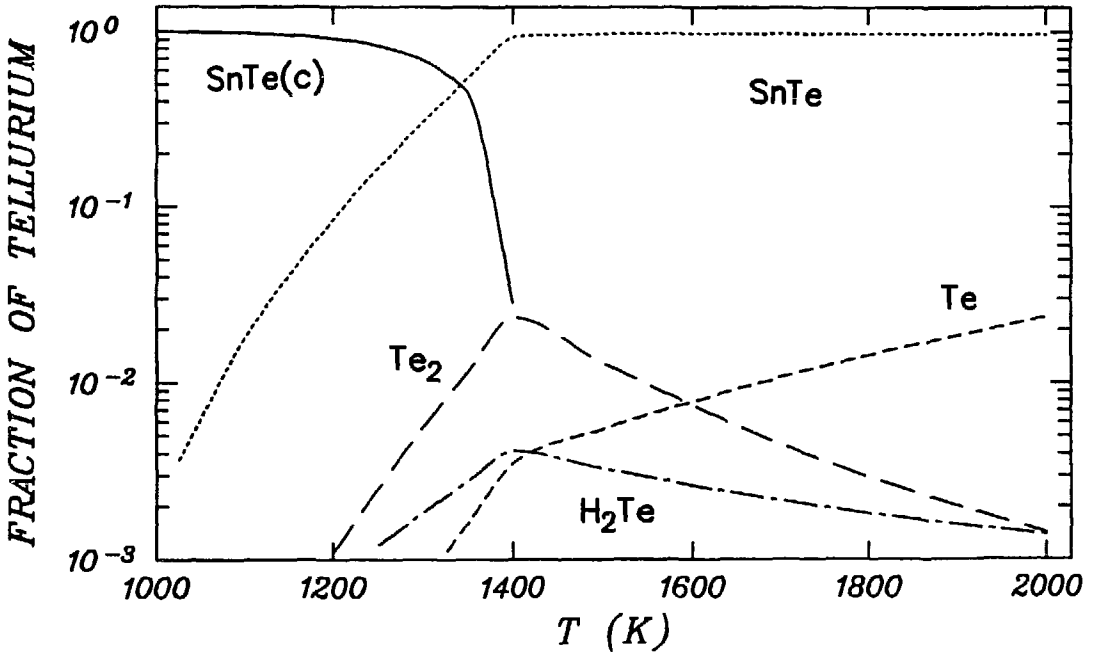

FIGURE 6: Tellurium Speciation Diagram in the Presence of Tin. The system contains 0.02 mol of tellurium, excess tin, 1 mol of steam, and 1 mol of hydrogen (H_2/H_2O = 1) at a pressure of 12 bar.

The addition of cesium changes the tellurium speciation even in the presence of tin because $Cs_2Te(c)$ is quite stable, especially at the lower temperatures. This is illustrated in Figure 7a, for the case Cs/Te = 4. (For values of Cs/Te less than 2, both $Cs_2Te(c)$ and SnTe(c) would be formed at low temperatures.) At high temperatures SnTe becomes the predominant tellurium gas-phase species. Figure 7b shows that the relative importance of SnTe increases if the Cs and Te abundances in the system are reduced.

The $SnTe/Cs_2Te$ ratio, at equilibrium, increases as the temperature or H_2O/H_2 ratio increase. This can be understood in terms of the equilibrium

$$Sn(c) + Cs_2Te + 2H_2O = SnTe + 2CsOH + H_2 \qquad (15)$$

An increase in the H_2O/H_2 ratio shifts the equilibrium of Reaction (15) to the right, increasing the $SnTe/Cs_2Te$ ratio. Furthermore, since the entropy change of Reaction (15) is positive, the Gibbs energy of Reaction (15) decreases with temperature (see Equation (14)), i.e., the formation of SnTe is more favourable at higher temperatures.

The equilibrium constant for Reaction (15) is given by

$$K_{15} = \frac{p(SnTe)p(CsOH)^2p(H_2)}{p(Cs_2Te)p(H_2O)^2} \qquad (16)$$

Approximate values of the $SnTe/Cs_2Te$ ratio at high temperatures can be obtained from Equation (16) by assuming that Cs_2Te, SnTe and CsOH are the only important tellurium and/or cesium species in the system. Using this assumption, we obtain the following implicit expression for y, the fraction of the tellurium in the form of Cs_2Te, i.e., $y = n(Cs_2Te)/N_T(Te)$,

$$(1 - y)\{N_T(Cs)/N_T(Te) - 2y\}^2F = yK_{15}/(N_T(Te))^2 \qquad (17)$$

where $F = p(H_2)[P_T/N_T p(H_2O)]^2$. The accuracy of this approximate expression improves as the temperature increases. Values of the ratio $SnTe/Cs_2Te$, which is equal to $(1 - y)/y$, are plotted in Figure 8 as a function of the Cs/Te ratio for various values of the temperature and tellurium abundance in the system ($N_T(Te)$).

The chemical speciation of tellurium in the presence of tin is affected by the addition of cesium (cf. Figures 6 and 7a). However, the total volatility of tellurium is not appreciably affected since (i) the vapour pressures of SnTe(c) and $Cs_2Te(c)$ are quite similar, and (ii) all the tellurium in the system is in the gas phase for temperatures above ~1300 K. Although the volatilities are similar, the calculated releases of tellurium (from containment) during a postulated reactor accident may still depend on the predominant tellurium compound formed in the PHTS,

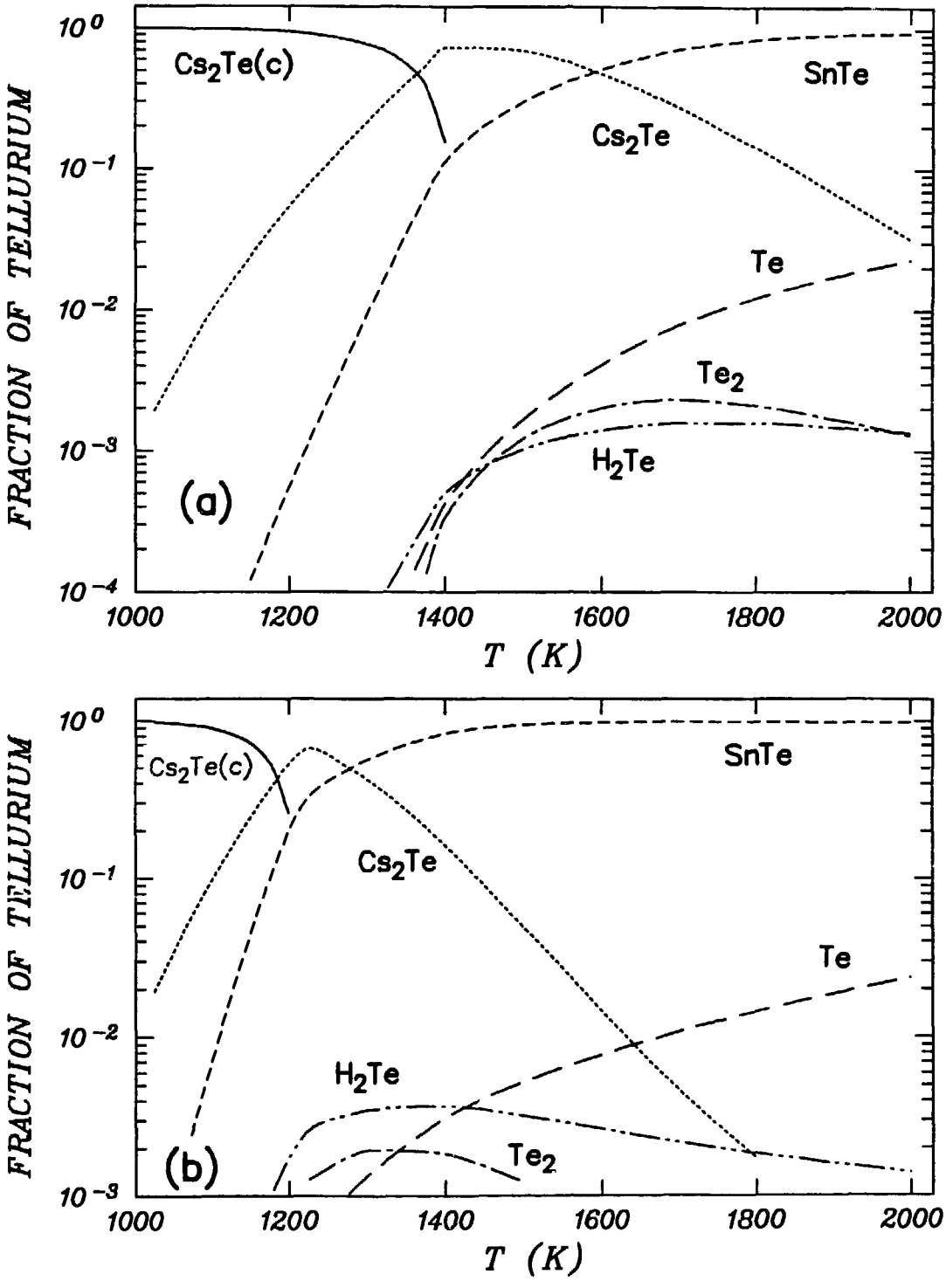

FIGURE 7: Tellurium Speciation Diagram in the Presence of Tin and Cesium. The system contains a 50% steam-hydrogen atmosphere (1 mol of steam), excess tin, cesium (Cs/Te = 4) and (a) 0.02 mol of tellurium or (b) 0.002 mol of tellurium.

since the physical and chemical properties of cesium telluride and tin telluride are different. For example, $Cs_2Te(s)$ is soluble in water whereas SnTe(s) is not very soluble, and Cs_2Te reacts readily with steam (see Equation (13)) whereas SnTe does not.

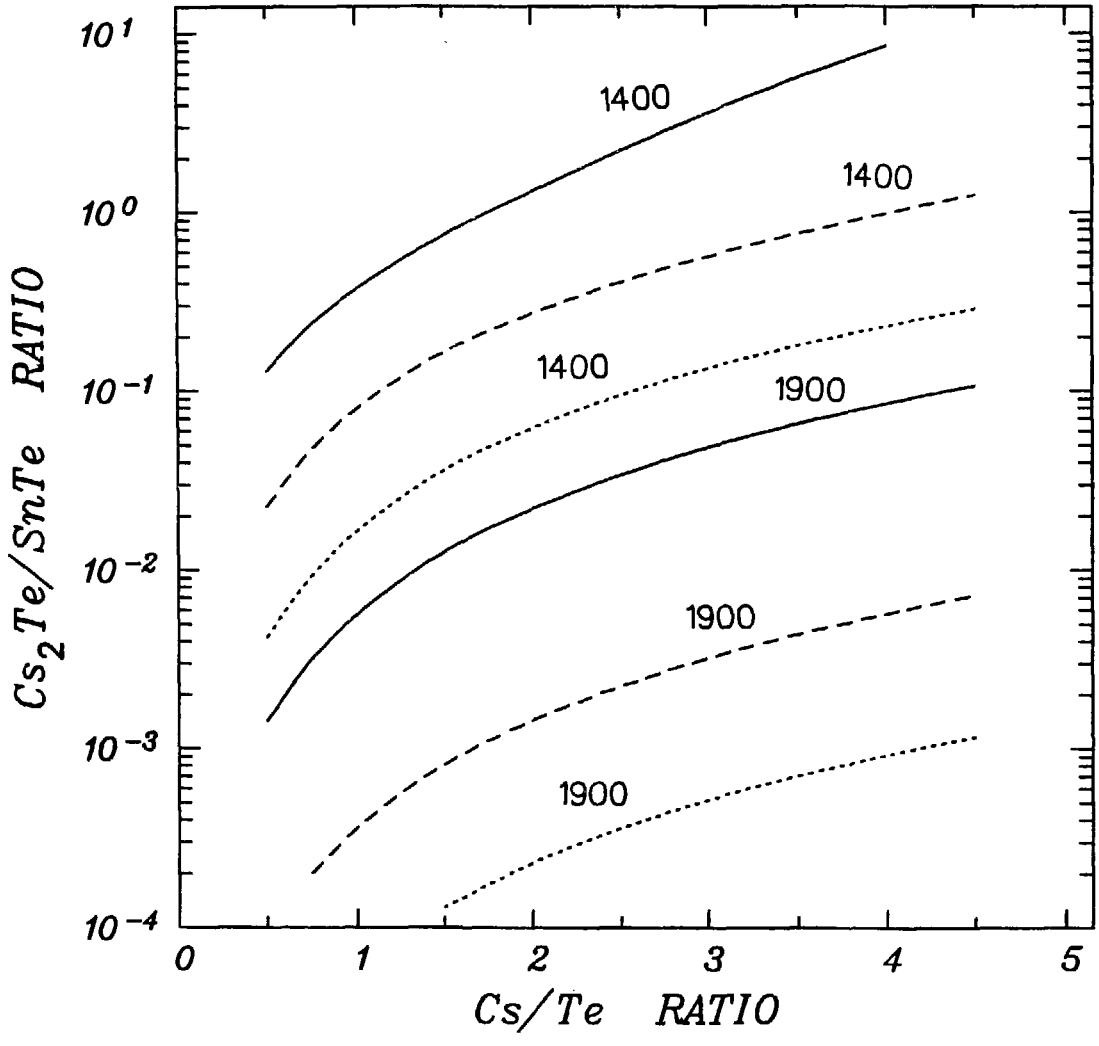

FIGURE 8: The $Cs_2Te/SnTe$ Ratio as a Function of the Cs/Te Ratio in a 50% Steam-Hydrogen Mixture (1 mol of steam) for Various Temperatures and Tellurium Abundances: (———) 0.02 mol of Te, (- - - -) 0.005 mol of Te, and (· · · ·) 0.002 mol of Te. The system pressure is 12 bar and the temperature is indicated in kelvin.

3.3.2 Tellurium Speciation in the Fuel Gap

In this section we investigate the behaviour of tellurium in the fuel-cladding gap. In this case Zircaloy is not oxidized and is available to react with tellurium. The inert filler gas and the fission product gases are the major gas-phase components in the fuel-cladding gap. Although chemical equilibrium calculations are done for temperatures up to 2000 K, this is not meant to imply that the fuel cladding would remain intact at these temperatures.

In the presence of the Zircaloy cladding (but no cesium), the thermodynamic calculations show that tellurium is tied up as $Zr_5Te_4(s)$, the Zr-Te compound with the largest Zr/Te ratio in the thermodynamic database. (The activity of Te in Zr is not presently available.) Under these conditions (see solid lines in Figure 9) Te is the most important tellurium gas-phase species and the volatility of tellurium is fairly low even at 2000 K. The vapour pressures of Te_2 and Te in the presence of $Zr_5Te_4(s)$ can be calculated using the equations in Table 4.

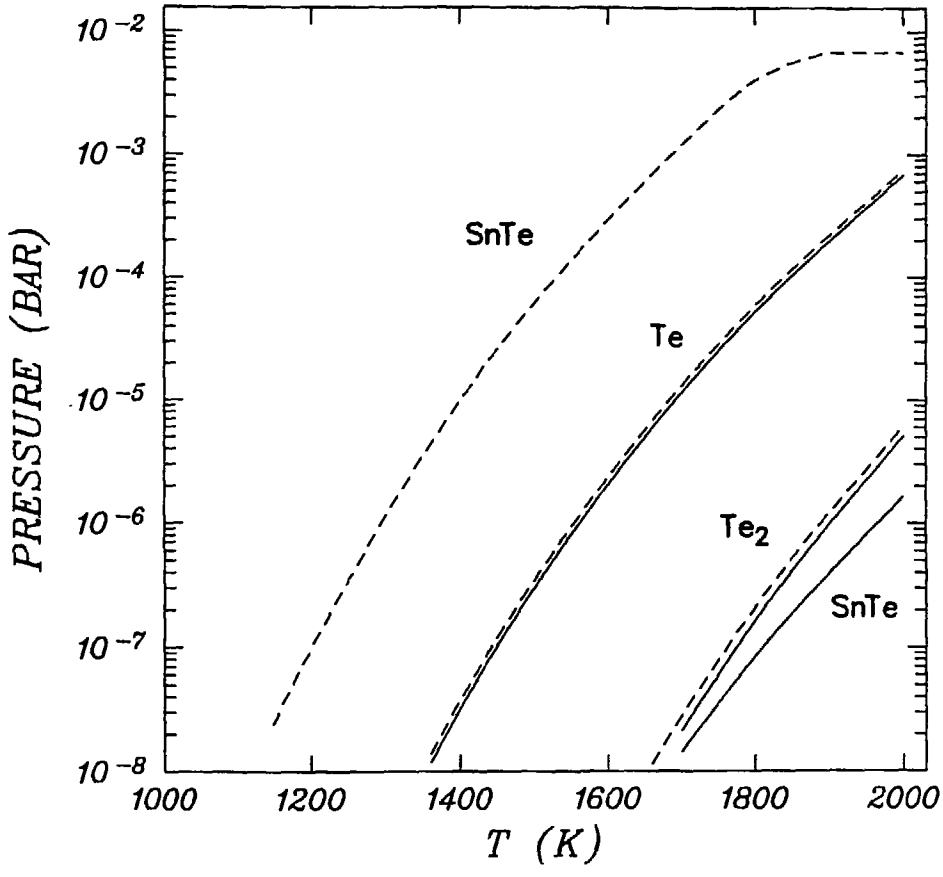

FIGURE 9: Tellurium Species Vapour Pressures in a System Containing 0.001 mol of Tellurium, Excess Zircaloy and Inert Gas (0.04 mol): (———) Alloy Model for Zircaloy and (- - - -) $SnZr_{99}(s)$ Model for Zircaloy. The major tellurium species (~100%) in the system is $Zr_5Te_4(s)$. The pressure is 25 bar.

The solid lines in Figure 9 were obtained using a Zr-Sn alloy model for Zircaloy (see Equation (8)), i.e., the other components of Zircaloy are ignored. For this model, the reaction of tellurium with Zircaloy forms $Zr_5Te_4(s)$ and the "excess" tin remains dissolved in the zirconium so that the tin fraction of the Zircaloy increases, e.g.,

$$SnZr_{99}(alloy) + 4w\ Te(c) = w\ Zr_5Te_4(s) + SnZr_{99-5w}(alloy) \qquad (18)$$

Although the alloy model of Zircaloy is the correct thermodynamic model, under some circumstances it may be desirable to model Zircaloy as a compound with a fixed stoichiometry, say $SnZr_{99}(s)$. The use of the $SnZr_{99}(s)$ model, for example, would allow release of tin during the Te-Zircaloy reaction:

$$SnZr_{99}(s) + 4w\ Te(c) = w\ Zr_5Te_4(s) + (1 - 5w/99)SnZr_{99}(s) + 5w/99\ Sn(c) \qquad (19)$$

The different behaviour illustrated in Equations (18) and (19) occurs even though the two Zircaloy models nominally have the same thermodynamic properties, e.g., the calculated Sn vapour pressure of Zircaloy is model-independent.

The effect of using a compound model for Zircaloy is shown by the dashed lines in Figure 9. The vapour pressures of Te and Te_2 are similar for both Zircaloy models. However, for the $SnZr_{99}(s)$ model, SnTe is the most important tellurium gas-phase species, and the total tellurium volatility, although low, is substantially greater than for the alloy model. This large difference between the two Zircaloy models arises because the activity coefficient of Sn in Zr is small and the fixed stoichiometry of $SnZr_{99}(s)$ forces the release of Sn(c) in Reaction (19). The dashed lines in Figure 9 were obtained using the following expression for the Gibbs energy of formation of $SnZr_{99}(s)$:

$$\Delta_f G^\circ(SnZr_{99}(s),T) = \Delta_f G^\circ(Sn(in\ Zr),T) + RT\ \ln(0.01) + 99\ \Delta_f G^\circ(Zr(s),T) \qquad (20)$$

where $\Delta_f G^\circ(Sn(in\ Zr),T)$ is defined in Equation (9).

The model that best represents the behaviour of Zircaloy during a particular postulated reactor accident probably depends on such non-thermodynamic factors as the mechanism of the Te-Zircaloy reaction and the anneal time after reaction. Although several studies of the tellurium-Zircaloy reaction exist in the literature [31,32,33], the experimental results are not always consistent. For example, Anand and Pruthi [33] observed a tin-rich layer after annealing Zircaloy-4 samples with tellurium (this would support the pure-compound model for Zircaloy), whereas this layer was not observed by Sallach et al. [32]. As always, the results of the thermodynamic calculations should be used with caution. This is particularly true for

transient conditions since, in this case, the assumption that the system has attained chemical equilibrium may not be valid, especially if gas-solid or solid-solid reactions are important.

The effect of adding cesium to the fuel gap is illustrated in Figure 10a and 10b for Cs/Te = 2 and Cs/Te = 3 respectively. The formation of cesium telluride is favoured, especially at low and intermediate temperatures,

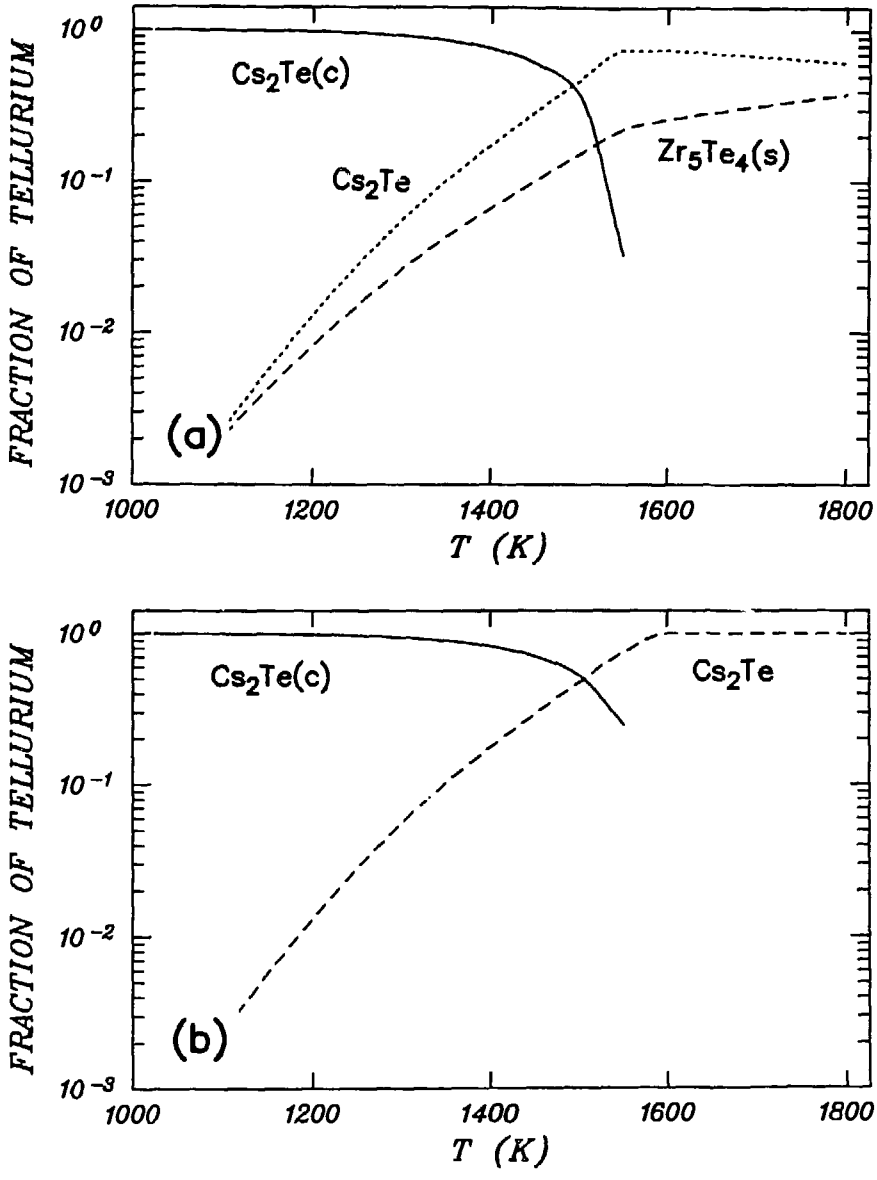

FIGURE 10: Tellurium Speciation Diagram in the Presence of Zircaloy and Cesium. The system contains tellurium (0.001 mol), excess Zircaloy, inert gas (0.05 mol) and cesium: (a) Cs/Te = 2 and (b) Cs/Te = 3. The pressure is 25 bar.

for high Cs/Te ratios, and high Cs and Te concentrations. More importantly, the presence of cesium in the fuel gap significantly increases the volatility of tellurium. The results presented in Figure 10 are in qualitative agreement with the observation that the "massive" deposits on the inside surfaces of boiling-water reactor (BWR) cladding have Cs/Te ratios of 2 [29]. A cesium telluride compound, CsTe, has also been observed in a mass spectrometric study of fission product releases from irradiated fuel [30].

The calculations presented in Figure 10 are valid for very low oxidation potentials since they neglect the possible formation of cesium uranates [34,35,36]. In order to illustrate the effect of higher oxidation potentials, chemical equilibrium calculations that include $UO_{2+x}(s)$ (modelled as an ideal solid solution of $UO_2(s)$ and $U_4O_9(s)$) and $Cs_2UO_4(s)$ have been done. (The other cesium uranates were not included in these scoping calculations.) The results of these calculations are shown in Figure 11. Comparison of Figures 10 and 11 shows that, at these higher oxidation potentials (about -330 $kJ \cdot mol^{-1}$), $Cs_2Te(s)$ is unstable with respect to formation of $Cs_2UO_4(s)$, and, concomitantly, $Zr_5Te_4(s)$ becomes the most important tellurium species below about 1550 K. Thus, the chemical speciation of tellurium in the fuel gap depends strongly on the oxidation potential of the fuel and, hence, the fuel burnup.

3.4 THERMODYNAMIC BEHAVIOUR OF TELLURIUM UNDER OXIDIZING CONDITIONS

Figure 3 shows the chemical speciation of tellurium in a 50% steam-air mixture in the absence of cesium. Figure 12 shows the chemical speciation of tellurium in a 50% steam-air atmosphere in the presence of cesium (Cs/Te = 2). At low and intermediate temperatures cesium tellurate and cesium tellurite, respectively, are the predominant tellurium species in the system. Cesium tellurates with lower Cs/Te ratios (e.g., $Cs_2Te_4O_9(s)$) could also form if the Cs/Te ratio in the system is less than 2. At the higher temperatures cesium tellurite decomposes and all the tellurium is in the gas phase.

The formation of cesium tellurate or cesium tellurite decreases the volatility of tellurium (cf. Figures 3 and 12). However, these compounds are made in the laboratory by heating (at ~500°C) mixtures of $TeO_2(s)$ and $Cs_2CO_3(s)$ in various molar ratios for many hours [37]. It is not known if these compounds can be formed in the PHTS under reactor accident conditions. Ignoring the formation of these compounds produces a conservative approximation, at least for those cases in which the calculated risk (dose) factors for tellurium are proportional to the volatility of tellurium.

The presence of tin would not affect the results presented in Figures 3 or 12 because tin telluride is unstable under oxidizing conditions. The Gibbs energy change for the reaction

$$SnTe + 2O_2 \rightarrow SnO_2(c) + TeO_2 \qquad (21)$$

is large and negative, i.e., $\Delta_r G$ = -583 $kJ \cdot mol^{-1}$ and -293 $kJ \cdot mol^{-1}$ at 600 and 1500 K respectively.

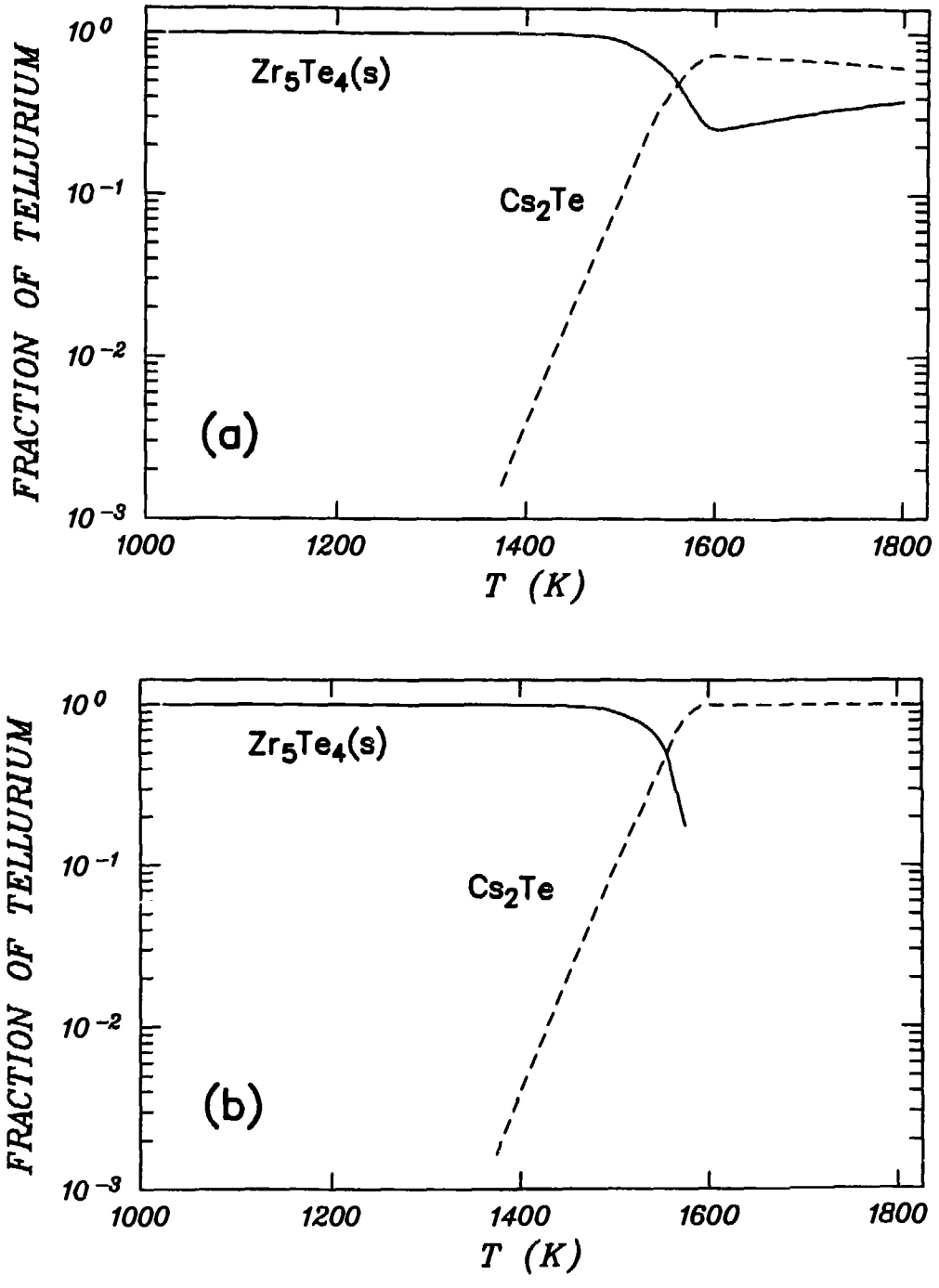

FIGURE 11: Tellurium Speciation Diagram in the Presence of Zircaloy, Cesium and UO_2 Fuel. The fuel is modelled as an ideal solution of $UO_2(s)$ and $U_4O_9(s)$, and the oxidation potential is -327 $kJ \cdot mol^{-1}$ at 1400 K. The system contains tellurium (0.001 mol), excess Zircaloy, inert gas (0.05 mol) and cesium: (a) Cs/Te = 2 and (b) Cs/Te = 3. The pressure is 25 bar.

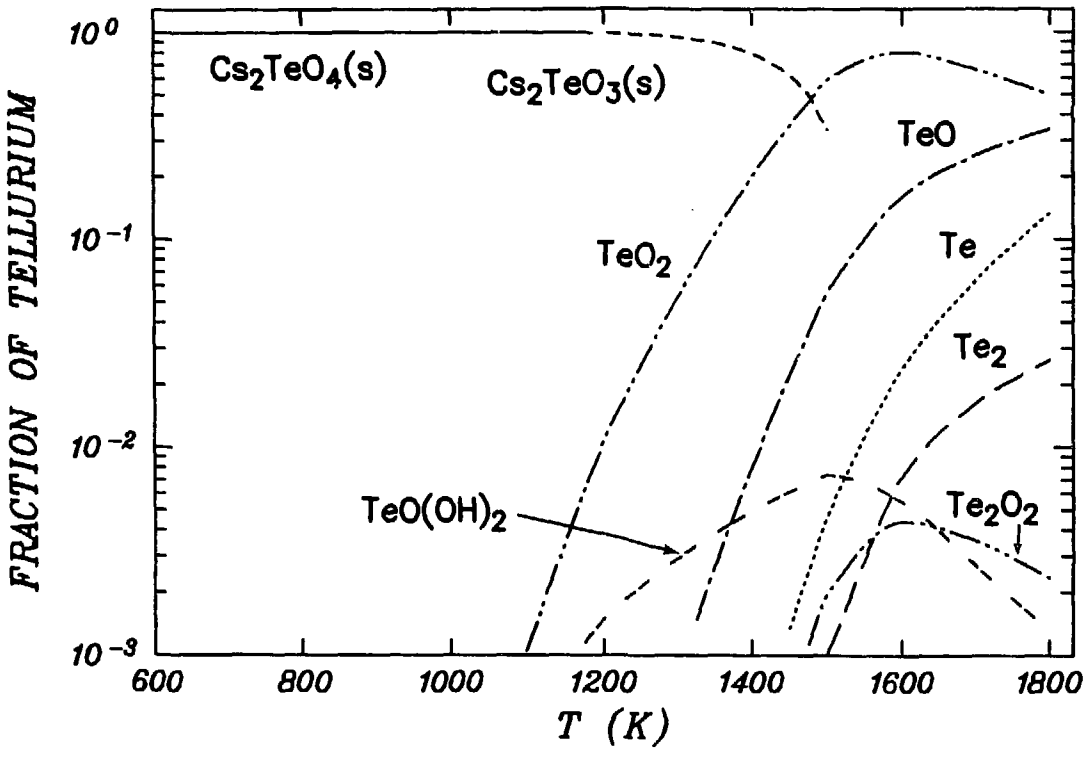

FIGURE 12: Tellurium Speciation Diagram for the Release of Tellurium (0.002 mol) and Cesium (Cs/Te = 2) into a 50% Steam-Air Atmosphere (0.08 mol of steam) at 1-bar Pressure

3.5 SENSITIVITY ANALYSIS

In contrast to our previous studies [2,3] of the thermodynamic behaviour of fission products, the present study suffers from the lack of a reliable thermodynamic database, that is, the thermodynamic data for the important tellurium species Cs_2Te and $Zr_5Te_4(s)$ have large uncertainties. Consequently, a few calculations were carried out to examine the sensitivity of the results presented in Sections 3.2 and 3.3 to the Gibbs energies of formation of Cs_2Te and $Zr_5Te_4(s)$. Only calculations in which Cs_2Te is stabilized (or Zr_5Te_4 is destabilized) were carried out, because the volatility of tellurium increases for these changes. If, for example, Cs_2Te is less stable than the data used in this report would indicate, then the calculations in this report give upper bounds for the volatility of tellurium.

If the Gibbs energy of formation for Cs_2Te is stabilized by 20 $kJ \cdot mol^{-1}$, then the vapour pressure of $Cs_2Te(c)$ would increase by a factor of exp(-20 000/RT). The chemical speciation of tellurium in the gas phase is also affected (cf. Figures 5a and 13), i.e., the relative amount of Cs_2Te increases. However, at the higher temperatures, the increased stability of Cs_2Te does not increase the total volatility of tellurium, since all the

tellurium in the system is already in the gas phase. The other calculations presented in Section 3.2 should be similarly affected by the stabilization of Cs_2Te.

Instead of decreasing the stability of $Zr_5Te_4(s)$ for the sensitivity calculations we have simply removed it from the database. In this case, $ZrTe_2(s)$ is formed in the fuel-cladding gap rather than $Zr_5Te_4(s)$. A comparison of Figures 9 and 14 shows, as expected, that the total volatility of tellurium increases. The dashed curve for SnTe in Figure 14 reaches a limit because of the finite amount of tin released in the reaction of tellurium with $SnZr_{99}(s)$ (see Equation (20)).

The few sensitivity calculations presented above show the importance of a reliable thermodynamic database. More experimental work is needed to identify the cesium telluride species that contribute significantly to the vapour pressure of $Cs_2Te(c)$, and to determine their thermodynamic properties. Moreover, a better description of tellurium speciation in the fuel gap requires information on the activity coefficient of Te in Zr, and the thermodynamic properties of the zirconium-tellurium compounds, e.g., $Zr_5Te_4(s)$.

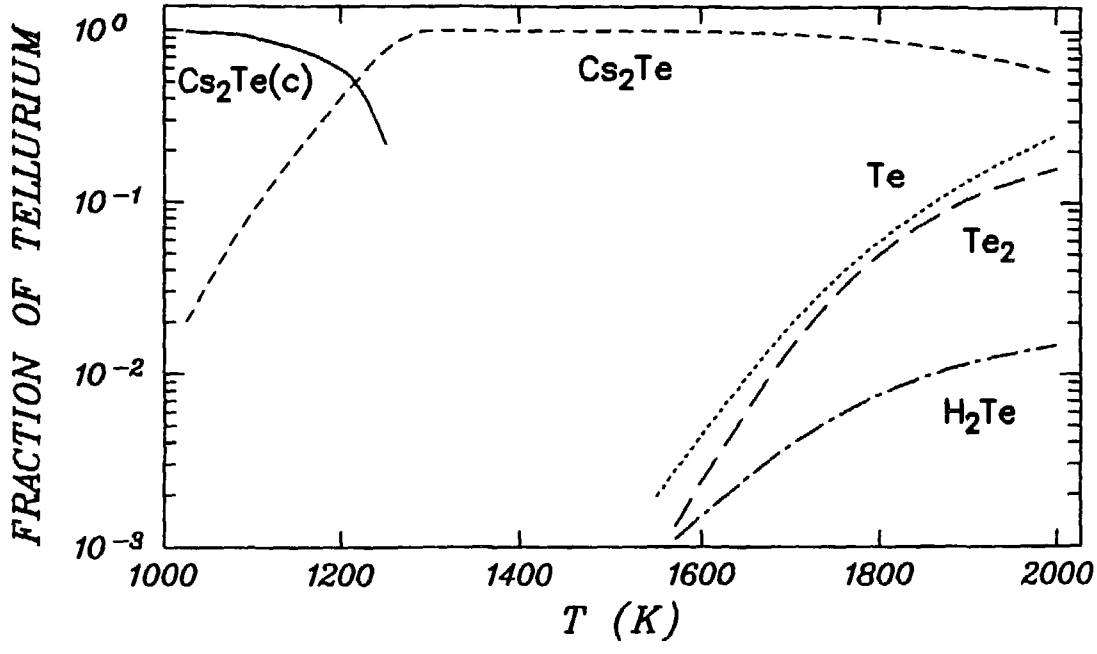

FIGURE 13: Tellurium Speciation Diagram for System Described in Figure 5a Except That the Gibbs Energy of Formation of $Cs_2Te(g)$ Is Decreased by 20 $kJ \cdot mol^{-1}$, i.e., Cs_2Te Is Stabilized with Respect to $Cs_2Te(c)$

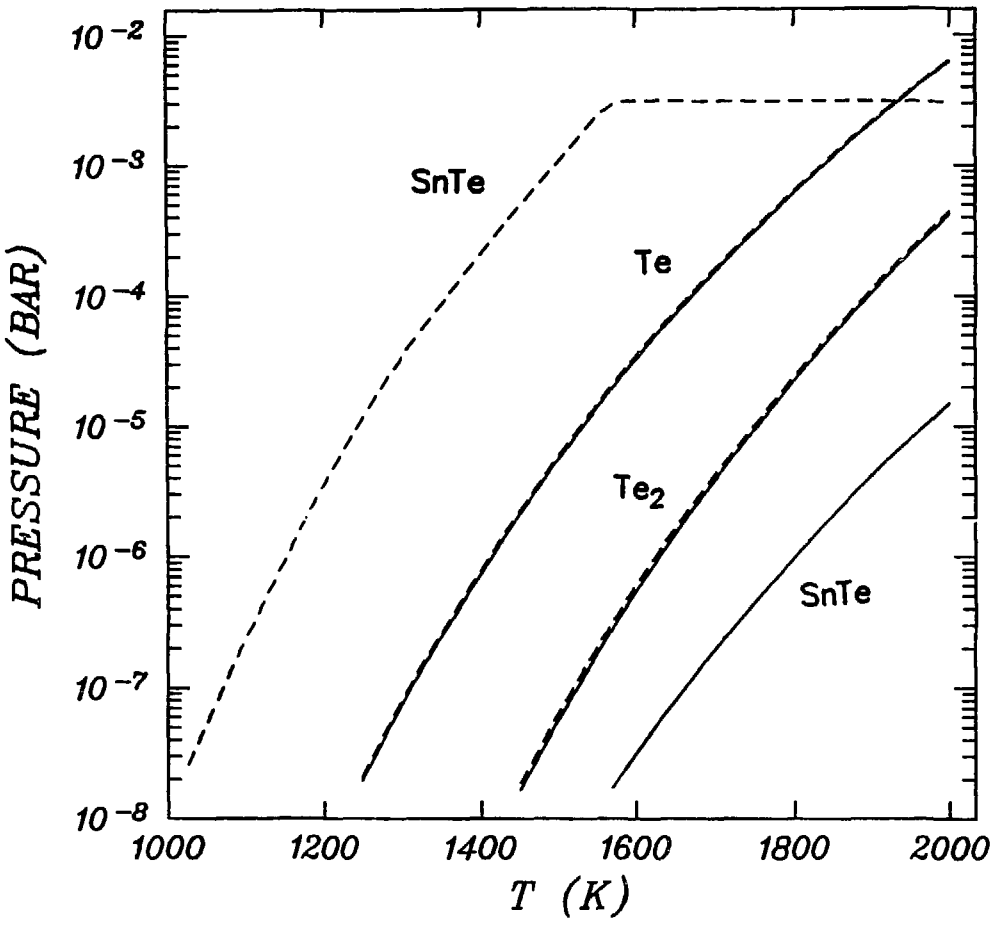

FIGURE 14: Tellurium Species Vapour Pressures for the System Described in Figure 9 Except That $Zr_5Te_4(s)$ Is NOT Included in the Calculations: (———) Alloy Model for Zircaloy and (- - - - -) $SnZr_{99}(s)$ Model for Zircaloy. $ZrTe_2(s)$ is the major tellurium species (~100%) in the system.

4. SUMMARY AND CONCLUSIONS

In this report chemical equilibrium calculations are used to predict the behaviour of tellurium in the PHTS under various postulated reactor accident conditions. A reliable and complete thermodynamic database is required to carry out these calculations. Unfortunately, for tellurium, not all the required thermodynamic data are available in the literature and it was necessary to use estimated data. Thus, the results presented in this report could change after new data become available for $Cs_2Te(g)$ and Te(in Zr).

The thermodynamic calculations in Section 3.3.2 show that the chemical form of tellurium in the fuel gap depends on the oxidation potential of the

fuel. For low oxidation potentials (i.e., cesium uranates are not formed), cesium telluride is stable, whereas for high oxidation potentials cesium telluride is unstable with respect to the formation of cesium uranates, and consequently $Zr_5Te_4(s)$ is formed in the fuel gap, i.e., tellurium is bound to the Zircaloy.

The formation of $Zr_5Te_4(s)$ in the gap could explain the observation [7,8,9] that tellurium releases from irradiated fuel are delayed until oxidation of the Zircaloy cladding is complete. If $Zr_5Te_4(s)$ is formed in the fuel gap, Figure 9 shows that the volatility of tellurium is low even at 2000 K. In this case, tellurium would be released slowly from failed fuel. However, the zirconium tellurides are unstable in the presence of steam. That is, the Gibbs energy change for the reaction

$$Zr_5Te_4(s) + 5H_2O \rightarrow 5ZrO_2(s) + 2Te_2 + 10H_2 \qquad (22)$$

is large and negative ($\Delta_r G$ = -1880 kJ·mol^{-1} at 1500 K). Thus, tellurium should be released rapidly after steam contacts the inside of the cladding.

The thermodynamic calculations also indicate that, after the cladding is oxidized, the tellurium in the PHTS could react with the liberated tin to form tin telluride (see Figures 6 and 7). Under these conditions, the important tellurium species (in the presence of cesium) would be $Cs_2Te(c)$ or Cs_2Te at low and intermediate temperatures respectively, and SnTe at high temperatures. Indirect evidence exists for the release of cesium telluride and tin telluride compounds from irradiated fuel [7,8,30].

Although the presence of tin will affect the chemical speciation of tellurium in the PHTS, the total volatility of tellurium is not much affected. This is because (i) SnTe(c) and $Cs_2Te(c)$ have similar vapour pressures, and (ii) all the tellurium is in the gas phase for temperatures above ~1300 K. However, the physical and chemical properties of cesium telluride and tin telluride are different. Thus, the releases of tellurium during a postulated reactor accident would, in principle, depend on the predominant tellurium compound formed in the PHTS.

In conclusion, we can state that much is known about the thermodynamic behaviour of tellurium in the PHTS under reactor accident conditions. However, more information is required on (i) the thermodynamic properties of the important cesium telluride gas-phase species; (ii) the thermodynamic properties of the Zr-Te system, in particular the activity coefficient of tellurium in zirconium-rich Zr-Te alloys; (iii) the chemical form of tellurium in the fuel; (iv) the mechanism and rate of the tellurium-Zircaloy reaction; and (v) the formation of (cesium) tellurates or tellurites under postulated reactor conditions. This information will lead to a better understanding of the chemistry of tellurium in the PHTS.

ACKNOWLEDGEMENT

This work was jointly funded by AECL Research and Ontario Hydro, Hydro Québec and the New Brunswick Electric Power Commission under the CANDU Owners Group (COG) program.

REFERENCES

1. R.A. Lorenz, J.L. Collins, A.P. Malinauskas, O.L. Kirkland and R.L. Towns, "Fission Product Release From Highly Irradiated LWR Fuel," Oak Ridge National Laboratory Report, ORNL/NUREG/TM-287/R2 (1980).

2. F. Garisto, "Thermodynamics of Iodine, Cesium and Tellurium in the Primary Heat-Transport System Under Accident Conditions," Atomic Energy of Canada Limited Report, AECL-7782 (1982).

3. F. Garisto, "Thermodynamic Behaviour of Ruthenium at High Temperatures," Atomic Energy of Canada Limited Report, AECL-9552 (1988).

4. D.J. Wren, "Kinetics of Iodine and Cesium Reactions in the CANDU Reactor Primary Heat Transport System Under Accident Conditions," Atomic Energy of Canada Limited Report, AECL-7781 (1983).

5. F. Garisto, F.C. Iglesias and C.E.L. Hunt, "A Thermodynamic/Mass-Transport Model for the Release of Ruthenium from Irradiated Fuel," in Fission Product Transport Processes in Reactor Accidents (editor J.T. Rogers), Hemisphere Publishing, New York, 1990, p. 257.

6. F.C. Iglesias, C.E.L. Hunt, F. Garisto and D.S. Cox, "Ruthenium Release Kinetics from Uranium Oxides," in Fission Product Transport Processes in Reactor Accidents (editor J.T. Rogers), Hemisphere Publishing, New York, 1990, p. 187.

7. J.L. Collins, M.F. Osborne and R.A. Lorenz, "Fission Product Tellurium Release Behavior Under Severe Light Water Reactor Accident Conditions," Nuclear Technology 77, 18-31 (1987).

8. M.F. Osborne, J.L. Collins and R.A. Lorenz, "Experimental Studies of Fission Product Release from Commercial Light Water Reactor Fuel Under Accident Conditions," Nuclear Technology 78, 157-169 (1987).

9. G. Le Marois and R. Warlop, "Source Term Experiment for Fission Product Transport: The HEVA Program," in Proceedings of the International ENS/ANS Conference on Thermal Reactor Safety, Avignon, France, 1988, Volume 1, p. 409.

10. E.H.P. Cordfunke and R.J.M. Konings (editors), Thermochemical Data for Reactor Materials and Fission Products, Elsevier Science Publishers, New York, 1990.

11. K.C. Mills, Thermodynamic Data for Inorganic Sulphides, Selenides and Tellurides, Butterworths, London, 1974.

12. V.P. Glushko (Corresponding Editor) et al., Thermodynamic Properties of Individual Substances, Vol. 1-4, Moscow Science Press, 1978-1982.

13. S.G. Frankiss and J.H.S. Green, "Statistical Methods for Calculating Thermodynamic Functions," in Chemical Thermodynamics, Vol. 1 (editor M.L. McGlashan), The Chemical Society, London, 1973, pp. 268-316.

14. R.H. Lamoreaux and D.L. Hildenbrand, "High Temperature Vaporization Behavior of Oxides. I. Alkali Metal Binary Oxides," Journal of Physical and Chemical Reference Data 13, 151-173 (1984).

15. G. Herzberg, Molecular Spectra and Molecular Structure: II. Infrared and Raman Spectra of Polyatomic Molecules, D. Van Nostrand, Princeton, New Jersey, 1966.

16. E.H.P. Cordfunke, F. Kleverlaan and W. Ouweltjes, "The Vapour Pressure of Di-Caesium Telluride (Cs_2Te)," Thermochimica Acta 102, 387-390 (1986).

17. R. Portman, M.J. Quinn, N.H. Sagert, P.P.S. Saluja and D.J. Wren, "A Knudsen Cell-Mass Spectrometer Study of the Vaporization of Cesium Telluride and Cesium Tellurite," Thermochimica Acta 144, 21-31 (1989).

18. S. Yamanaka, N. Takatsuka, M. Katsura and M. Miyake, "Study of the Zr-Te-O Ternary System," Journal of Nuclear Materials 161, 210-215 (1989).

19. S. Yamanaka, M. Katsura and M. Miyake, "An Estimation of Thermodynamic Stability of Zirconium Tellurides," Technology Reports of Osaka University 38, No. 1915, p. 59, March 1988.

20. R.H. Zee, J.F. Watters and R.D. Davidson, "Diffusion and Chemical Activity of Zr-Sn and Zr-Ti Systems," Physical Review B34, 6895-6901 (1986).

21. A.K. Niessen, F.R. de Boer, R. Boom, P.F. de Chatel, W.C.M. Mattens and A.R. Miedema, "Model Predictions for the Enthalpy of Formation of Transition Metal Alloys II," CALPHAD 7, 51-70 (1983).

22. O. Kubaschewski and C.B. Alcock, Metallurgical Thermochemistry, 5th edition, Pergamon Press, Oxford, 1979.

23. W.R. Smith and R.W. Missen, Chemical Reaction Equilibrium Analysis: Theory and Algorithms, John Wiley & Sons, New York, 1982.

24. V.F. Urbanic and T.R. Heidrick, "High-Temperature Oxidation of Zircaloy-2 and Zircaloy-4 in Steam," Journal of Nuclear Materials 75, 251-261 (1978).

25. J.W. Mellor, A Comprehensive Treatise on Inorganic and Theoretical Chemistry, Volume XI (Te, Cr, Mo, W), Longmans, London, 1931.

26. A.P. Malinauskas, J.W. Gooch Jr. and J.D. Redman, "The Interaction of Tellurium Dioxide and Water Vapor," Nuclear Applications and Technology 8, 52 (1970).

27. S. Imoto and T. Tanabe, "Chemical State of Tellurium in a Degraded LWR Core," Journal of Nuclear Materials 154, 62-66 (1988).

28. D. Cubicciotti and J.E. Sanecki, "Characterization of Deposits on Inside Surfaces of LWR Cladding," Journal of Nuclear Materials 78, 96-111 (1978).

29. A. Ohuchi, "Characterization of Fission Product Deposits on Inside Surfaces of BWR Cladding," in Proceedings of IAEA Technical Committee Meeting on Fuel Rod Internal Chemistry and Fission Products Behaviour, Karlsruhe, 1985, p. 55, IWGFPT-25 (1986).

30. I. Johnson and C.E. Johnson, "Mass Spectrometry Studies of Fission Product Behavior: I. Fission Products Released from Irradiated LWR Fuel," Journal of Nuclear Materials 154, 67-73 (1988).

31. B.R. Bowsher, S. Dickinson, R.A. Gomme, R.A. Jenkins, A.L. Nichols and J.S. Ogden, "The Interaction of Zircaloy Cladding with Fission Product Tellurium Released During a Severe Reactor Accident," in Chemical Reactivity of Oxide Fuel and Fission Product Release, Proceedings of Conference (K.A. Simpson and P. Wood editors), Berkeley Nuclear Laboratories, 1987, p. 455.

32. R.A. Sallach, C.J. Greenholt and A.R. Taig, "Chemical Interactions of Tellurium Vapors with Reactor Materials," Nuclear Regulatory Commission Report, NUREG/CR-2921 (1984).

33. M.S. Anand and D.D. Pruthi, "Surface Reactions of Tellurium on Steel and Zircaloy-4," Government of India Atomic Energy Commission, Bhabha Atomic Research Centre Report, BARC-1009 (1979).

34. D.C. Fee and C.E. Johnson, "The Interaction of Cesium with Urania in Uranium-Plutonium Oxide Fast Reactor Fuel Pins," Journal of Nuclear Materials 78, 219-224 (1978).

35. K. Une, "Reactions of Cesium with Nonstoichiometric $UO_{2\pm x}$ and $U_{0.86}Gd_{0.14}O_{2\pm x}$ Pellets," Journal of Nuclear Materials 144, 128-140 (1987).

36. R.G.J. Ball, W.G. Burns, J. Henshaw, M.A. Mignanelli and P.E. Potter, "The Chemical Constitution of the Fuel-Clad Gap in Oxide Fuel Pins for Nuclear Reactors," Journal of Nuclear Materials 167, 191-204 (1989).

37. E.H.P. Cordfunke and V.M. Smit-Groen, "A DSC Study of the Phase Diagram of the System TeO_2-Cs_2TeO_3," Thermochimica Acta 80, 181-183 (1984).

ISSN 0067-0367

To identify individual documents in the series, we have assigned an AECL- number to each.

Please refer to the AECL- number when requesting additional copies of this document

from

Scientific Document Distribution Office
AECL Research
Chalk River, Ontario, Canada
K0J 1J0

Price: A

ISSN 0067-0367

Pour identifier les rapports individuels faisant partie de cette série, nous avons affecté un numéro AECL- à chacun d'eux.

Veuillez indiquer le numéro AECL- lorsque vous demandez d'autres exemplaires de ce rapport

au

Service de Distribution des Documents Scientifiques
EACL Recherche
Chalk River, Ontario, Canada
K0J 1J0

Prix: A